AD-774 450

STUDIES OF ATMOSPHERIC PROCESSES

Edward R. Fisher, et al

Wayne State University

Prepared for:

Air Force Cambridge Research Laboratories
Advanced Research Projects Agency

15 June 1973

Program code numbers............................ 2E40

Effective date of contract...................... 12 July 1971

Contract expiration date........................ 31 December 1973

Co-Principal Investigators & phone Nos.......... Dr. A.R. Hochstim
(313) 577-3867

Dr. E.R. Fisher
(313) 577-3896

Project Scientist or Engineer & phone No........ Dr. A.T. Stair
(861) 617-4911

AD 744 450

REPORT DOCUMENTATION PAGE		READ INSTRUCTIONS BEFORE COMPLETING FORM
1. REPORT NUMBER Semi-Annual Report No. 4	**2. GOVT ACCESSION NO.**	**3. RECIPIENT'S CATALOG NUMBER**
4. TITLE (and Subtitle) Studies of Atmospheric Processes		**5. TYPE OF REPORT & PERIOD COVERED** 12/15/72-6/15/73 Semi-Annual
		6. PERFORMING ORG. REPORT NUMBER
7. AUTHOR(s) Edward R. Fisher Richard Marriott Ralph H. Kummler Pieter Rol		**8. CONTRACT OR GRANT NUMBER(s)** F19628-72-C-0007
9. PERFORMING ORGANIZATION NAME AND ADDRESS Research Institute for Engineering Sc. Wayne State University Detroit, Michigan 48202		**10. PROGRAM ELEMENT, PROJECT, TASK AREA & WORK UNIT NUMBERS** Project No. 8692
11. CONTROLLING OFFICE NAME AND ADDRESS Defense Advanced Research Projects Ag. 1400 Wilson Blvd. Arlington, Virginia 22209		**12. REPORT DATE** June 15, 1973
		13. NUMBER OF PAGES
14. MONITORING AGENCY NAME & ADDRESS(if different from Controlling Office) Air Force Cambridge Research Labs. AFSC H Q Hanscom Field Bedford, Mass. 01730		**15. SECURITY CLASS. (of this report)** unclassified
		15a. DECLASSIFICATION/DOWNGRADING SCHEDULE

16. DISTRIBUTION STATEMENT (of this Report)

unlimited

17. DISTRIBUTION STATEMENT (of the abstract entered in Block 20, if different from Report)

unlimited

18. SUPPLEMENTARY NOTES

19. KEY WORDS (Continue on reverse side if necessary and identify by block number)

plume chemistry, energy transfer processes, chemi-luminescent processes

20. ABSTRACT (Continue on reverse side if necessary and identify by block number)

The Research Institute for Engineering Sciences at Wayne State University has been involved in characterizing the important radiation producing chemistry associated with fuel afterburning in the atmosphere. The radiation signatures (stressing the infrared spectral region) from fuel combustion in the atmosphere at high altitudes are believed to be strongly affected by chemiluminescent processes involving reactions between radical species produced in chain reactions initiated

DD FORM 1 JAN 73 **1473** EDITION OF 1 NOV 65 IS OBSOLETE

species produced in chain reactions initiated by atmospheric oxygen atoms with fuel constituents. The output of these chemical studies are input to chemistry models which are used in the analysis and correlation of test results.

This semi-annual report details the currrent results obtained in experimentally and theoretically understanding the important radiation producing chemistry of high altitude fuel afterburning. The first section summarizes the experimental investigation of infrared chemiluminescence associated with oxygen atom attack of fuel species in the Flow Discharge Facility. The second section presents the results of experimental beam measurements of the intermolecular potentials of oxygen atom collisions with various plume species for use in theoretical calculations of vibrational excitation. The vibrational excitation calculations are summarized in section three of this report. (M)

Table of Contents

iii.

PART I: Infrared Chemiluminescence from Oxygen
          Atom Attack on Fuel Species.

     R H.Kummler and E R Fisher

iV,

INTRODUCTION

The energy released in an exothermic chemical reaction can
take several forms depending on the reaction path. The chemical
energy of the reactants can be converted into translational
energy of the products or it can be converted into internal
energy of the products or some combination of both. The
internal energy can be distributed among the electronic,
vibrational, or rotational modes of the product molecule or
molecules. If the product is elevated to a quantum state which
has an optically allowed transition to a lower state, then the
resulting light emitted permits the study of the reaction path
leading to the internal energy. The observation of radiation
associated with this non-equilibrium process thus provides
information regarding the fundamental chemical kinetics of
the reaction (e.g., Charters and Polanyi (1960); Polanyi, 1966:
Pacey and Polanyi, 1971; Kushafar, et al, 1971). It also
provides the opportunity to assess the presence of one or both
of the reactant partners in an unknown mixture of reactant gases.

This capability is of considerable interest in the air pollution
monitoring field and is applicable to both local and remote monitoring
of exhaust gases (of rockets as well as automobiles) in the presence
of an oxygen atom enviroment. In the spectral region of wave-
lengths from 1μ to roughly 20 or 30μ, the emitted light generally
characterizes vibrational transitions which can result when the
exothermic reaction produces a new bond in a heteronuclear molecule.

1

In previous work (Krieger, Malki, and Kummler, 1972; Malki, 1972; Krieger and Kummler, 1973) we have investigated the light emitted by reactions which might be expected to occur under conditions appropriate to hydrocarbon combustion in the upper atmosphere. First, we identified the potential radiatiors on the basis of the known ground state chemistry and energetics. Second, we identified the visible and near infrared (7000-9000A) emission which illustrated the presence of both electronically and highly vibrationally excited OH early in the reactor time scale. Third, we estimated the quantum yield for the emission of photons at 2.7μ (Kummler, Fisher, and Malki, 1973) using non-dispersive techniques for $O+C_2H_4$. While the indirect evidence appeared to strongly support OH as the radiating species in all of the previous work, we had not been able to obtain the direct spectral evidence needed to positively identify the radiator. In this work, we have concentrated on providing the spectroscopic measurements necessary to achieve the identification for a variety of potentially important systems:

(1) $O+C_2H_4$ (6) $O+C_2H_6$

(2) $O+C_2H_2$ (7) $O+C_4H_{10}$

(3) $H+NO_2$ (8) $O+C_3H_6$

(4) $O+HCHO$ (9) $OH+CO$

(5) $H+HO_2$ (10) $OH+C_2H_4$

2

EXPERIMENTAL PROCEDURE

All experiments were conducted at roughly 1 Torr total pressure using a discharge flow system shown schematically in Figure (1). This system is very similar to that previously decribed by Krieger, Malki and Kummler (1972) and by Malki (1972). For convenience we will repeat that description as follows.

The flow tube reactor is a 4 ft. long stainless-steel tube with a 1 inch I.D. teflon tube liner which aids in preventing wall recombination of some atomic species. It is provided with six ports for radial viewing through quartz windows (Muffaletto Optical Company, Baltimore, Md.) Two additional ports were used for measuring the absolute pressure and the drop in pressure across the reactor. Linear average velocities up to 80m/sec(with 70 m/sec being a typical velocity) were achieved when the pressure in the reactor was about 1 torr using a Heraeus Englehard (E-225, 147 cfm) mechanical pump and Roots Blower.

A Baratron (MKS type 77) capacitance manometer with a three Torr head was employed to monitor the reactor pressure to better than 0.1μ accuracy. An alphatron (type 520) and a transducer (Viatran model 304, 0 - 15 psia) were the pressure sensing devices used to monitor ballast tank pressures. Their respective locations and functions in the system are illustrated (as well as other equipment) in Table (1).

The detectors used for this work are the PbS detector (Santa Barbara Research ITO type) in conjunction with a phase sensitive lock-in amplifier (PAR HR-8) for IR detection, and the photomultiplier detector (RCA C31025C) in conjunction with an electrometer (Keithley 602) for detection of visible emission.

3

Figure 1. Schematic of Flow System. M is a mount for the PbS detector (P), supplied by a high voltage power supply (Hi), E is the PAR HR8 phase sensitive lock in amplifier, and R is the recording system.
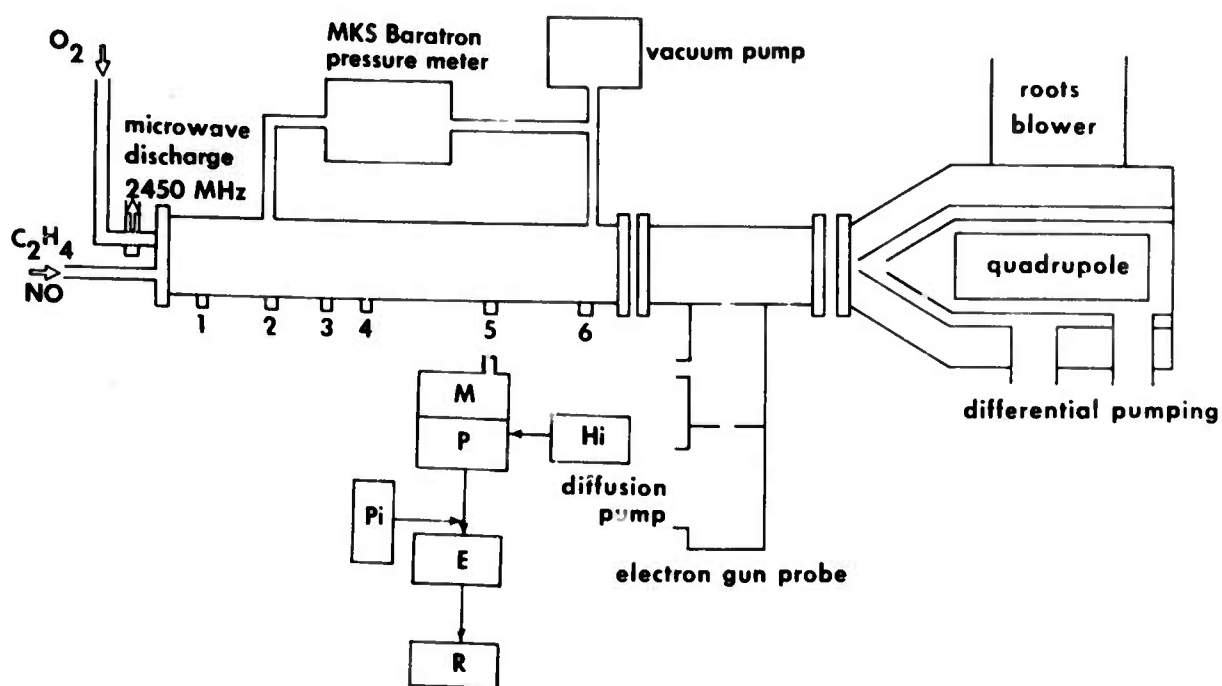

Fig.1 -Schematic of Discharge Flow Tube Reactor and Detection System

Table I

Equipment Itemization

| Category	Equipment	Make & Model	Specifications	Comments
P Measuring	Baratron	MKS (type 77)	1μ is read with 1% accuracy. 0-10 Torr.	A variable capacitance sensor measures pressure independent of the kind of gas. P fluctuations limit accuracy to 1μ.
	Alphatron	(type 520)	5% accuracy 0-1 atm.	α particle ionization head measures the pressure (see calibration, Appendix V).
	Transducer	Viatran (Model 304)	Range (0-15 psia); sensitivity, 1 Torr	
Recorders	X-Y Recorder	Honeywell (Model 560)	Range (50μv-50V)	
	Chart Recorder	Honeywell (Electronic 194)	Range (0.1mv-150v)	Chart speed 10 min/in to 1 sec/in two channels.
Power Generator	Pulsed Microwave Power Generator	Raytheon (Model PGM 10x2)	Input (105-130v), 60 cycle, 385W. Variable output up to 85 watts at 2750 MHz.	A pulsed system with an Evansen type cavity.

Table I (Continued)

Equipment Itemization

Category	Equipment	Make & Model	Specifications	Comments
Amplifiers	High Voltage Supply	Keithley	200-2200 volts	
	High Voltage Supply	Pacific Design	1-2000 volts, 10 MA.	
	Phase Sensitive Lock-In Amp	PAR (HR8)	100nv-500mv, range. Time constant, 1 m sec-100 sec.	Provides phase sensitive detection for recovery of weak signals.
	Low Noise Amplifier	PAR (113)	Full output voltage to 300 KHz.	
Detectors	PBS Detector	Santa Barbara Research Center (type 8471, ATO)		Used for infrared detection.
	Photomultiplier	RCA (Model C31025C)	Spectral response range (200-916 manometers).	Used for visible observations.
	Photomultiplier	RCA (1P28)		Used for O titration.
Filters	2.7μ Filter	Optical Cooling lab	See transmission Appendix I	Used for OH‡ observations.
	.678μ Shortwave cut off filter	Corning (CSN, 258)	Appendix I	Used for O titrations.

6

Table I (Continued)

Equipment Itemization

Category	Equipment	Make & Model	Specifications	Comments
	.610μ Shortwave cut off filter	Corning (CSN, 262)		Used for O titrations.
Oscilloscope	Oscilloscope	Techtronics 556	Dual beam type instrument, provides accurate voltage and time measurements. Complete independent operations of two beams.	Used for velocity measurements.

In order to get absolute emission values, the system had to be calibrated using the reaction (Fontijn et al, 1964)

$$NO + O \rightarrow NO_2 + h\nu \ (2.7\mu)$$
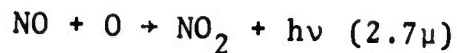
The actinometric standard of Fontijn, et al was extended into the 2.7μ region using the data of Kaufman (1973).

The oxygen atoms were generated by passing oxygen (Cryogenic sales 99.6%) pure or diluted in He (Cryogenic sales 99%) through an Evansen type cavity discharge powered by a 2450 MHz Raytheon PGM 10X2 diathermy unit.

The oxygen atoms were passed into the flow tube reactor through a closed end teflon tube with a radially multi-perforated exit stream. This permitted thorough mixing and a plug flow pattern at the point of mixing due to the turbulence caused by introducing the gas through a "showerhead" gas inlet. The plug on the end of the teflon piece served also to prevent the discharge region radiation from reaching the observation ports through scattering. The oxygen atom concentrations were measured by using the NO_2 titration technique (Kaufman 1964).

A steady state flow of the gas typical of the experiment (O_2 or O_2 + He or H_2 + He) was obtained. Then the microwave generator was turned on. Argon or Helium is usually used to keep the free atoms and radicals at low combinations , thus preventing recombination. It helps stabilize the discharge and it also served to keep the pressure in the reactor constant allowing a reasonably constant linear velocity upon adding the ground state gas.

8

Helium contributes most of the pressure in the reactor (~ 1 torr) while the ground state stream (NO, NO_2, C_2H_4, etc.) and the O_2 or H_2 are relatively small fractions of the total pressure.

The phase angle on the lock-in amplifier changed as one moved the PbS detector downstream and as the pressure changed in the flow tube. This had to be checked for all experimental data points. The reference to the PAR was taken from the pulse generator of the PGM 10X2. The pulse rate of the discharge was adjusted so that a single pulse of atoms traveled down the flow tube. This typically required repetition rates of 34 Hz to 100 Hz. The duty cycle for most measurements was 50%.

A pressure base line and a zero intensity base line were recorded on a two channel Honeywell electronic 194 recorder. As the ground state gas was added to the reactor, the intensity of the light emitted from the excited species was recorded with the corresponding preset scale on the lock-in amplifier. Utilization of the capillary flow meter permitted direct measurements of the intensity vs. upstream pressure at the capillary using the PAR, the Viatran pressure transducer and a Honeywell Model (56)) XY recorder.

A run that involved the reaction $NO + O \rightarrow O_2 + h\nu$ accompanied every set of data to put the lock-in amplifier readings on an absolute basis. A titration for oxygen atoms was also done as a part of the system calibration. The PbS detector with the PAR HR8 was used to monitor the intensity peak of the reaction $NO_2 + O \rightarrow NO + O_2$ as a function of NO_2 concentration.

THE MECHANISMS

A. $O + C_2H_4$ and $O + HCHO$
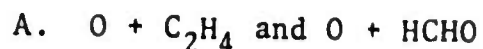
The mechanism for oxygen atom attack on ethylene is well established in terms of ground state chemistry and Malki (1972) has investigated the emission at 2.7μ in considerable detail.

The reaction of oxygen atoms with ethylene has been phenomenologically found to produce infrared radiation, at least partly in the 2.7μ region (Malki, 1972). The major effort of this work is devoted to the qualitative explanation of that radiation in terms of detailed spectra on which to base molecular mechanisms. The general ground state system of intermediates resulting from the combination of O and C_2H_4 is well established primarily from the discharge-flow-tube-time-of-flight mass spectrometric study of Niki et al (1969) and the direct observation of the products CH_3 and CHO in the high intensity crossed beam experiment of Kanofsky et al (1972). These two studies along with the similar flow tube mass spectrometric work of Herron and Penzhorn (1969) have established that the primary elementary step (90%) in the reaction mechanism is

$$O + C_2H_4 \rightarrow CH_3 + CHO \tag{1}$$

The eventual stable products formed by secondary reactions include H_2CO, CO, H_2, O_2, and H. Consideration of the temporal behavior of these products as well as isotopic experiments led Niki, et al (1969) to postulate that the following reactions occur:

$$CH_3 + O \rightarrow HCHO + H \tag{2}$$

$$CHO + O \rightarrow CO + OH \tag{4}$$

$$HCHO + O \rightarrow CHO + OH \tag{17}$$

10

$$CHO + O \to CO_2 + H \tag{5}$$

$$OH + O \to O_2 + H \tag{6}$$

$$CHO + H \to H_2 + CO \tag{7}$$

Water was not observed to be a product of this system by Niki but his system employed very small concentrations of C_2H_4 with O in excess, so that the OH concentration and hence the rate of the reaction:

$$OH + OH \to H_2O + O \tag{11}$$

were both small. In a more general case, H_2O might be a significant product, and it could be a significant radiator as well.

Both OH and H_2O are produced by exothermic reactions in the above sequence under conditions where each is the new bond formed by a neutral rearrangement reaction. Under conditions such as this, it is well established that a significant fraction of the exothermicity of the reaction can appear as vibrational energy in the new bond (Smith (1972); Pacey and Polanyi (1971); McGrath and Norrich (1957); Parker and Pimentel (1969); Jonathan, et al (1971); Stair and Kennealy (1967); Hushfar, et al (1971) and many others).

The Basic mechanism is illustrated in Figure 2 and detailed in Table II.
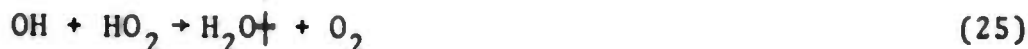
OXYGEN ATOM ATTACK ON ETHYLENE
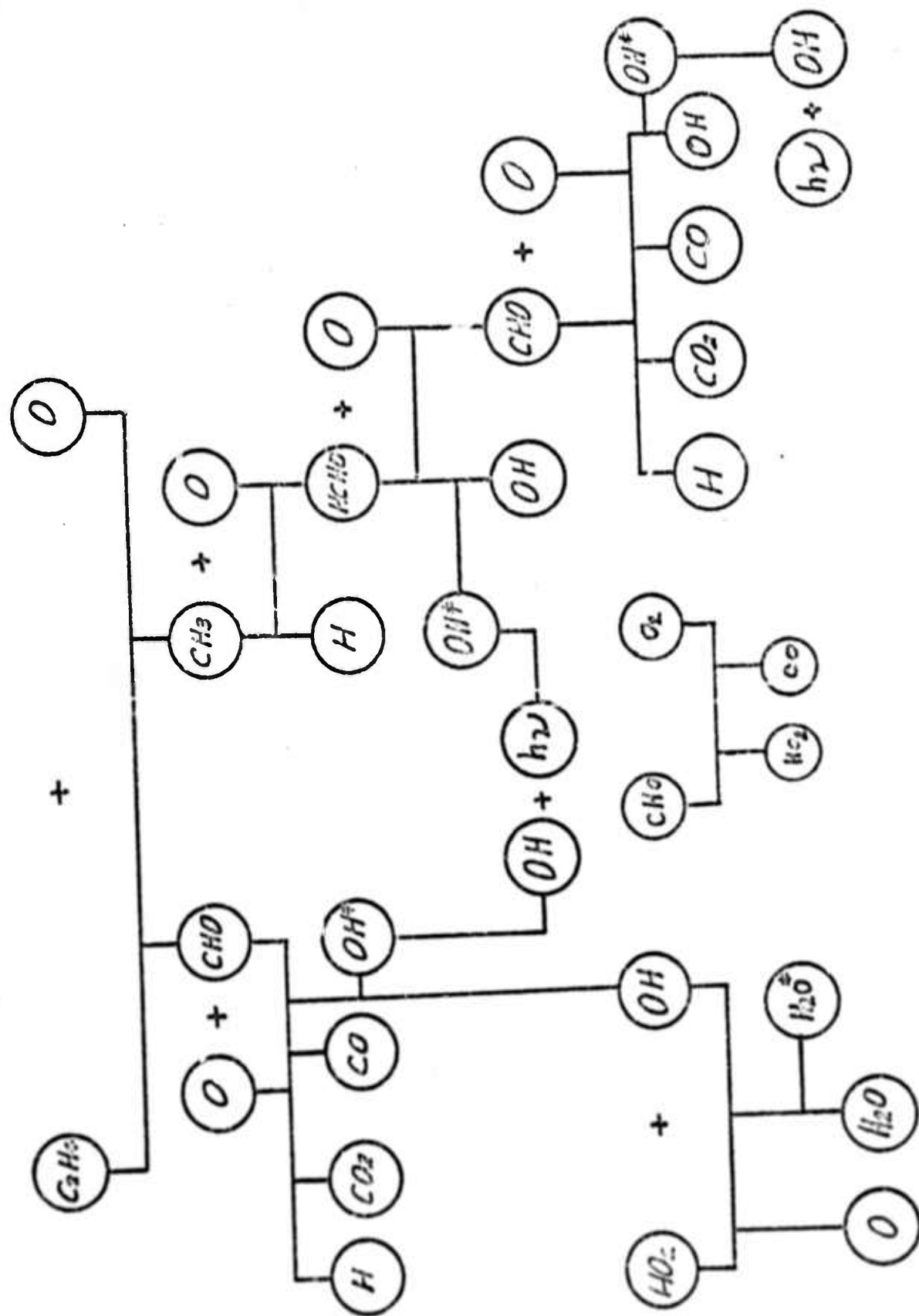
Figure 2. Schematic of the Reaction Mechanism Proposed

12

TABLE II (from Malki, 1972)

Reaction	Rate Constant $300^\circ K$	Reference	$\Delta H_r \frac{k\ cal}{gmole}$
1. $C_2H_4 + O \rightarrow CH_3 + CHO$	8.42^{-12}	Davis, et al (1972)	-42.45
2. $CH_3 + O \rightarrow HCHO + H$	3.0^{-11}	Niki, et al (1969)	-66.54
3. $HCHO + O \rightarrow CHO + OH\dagger$		Calculated	
4. $CHO + O \rightarrow OH$	1.0^{-12}	Niki, est.	-73.09
5. $CHO + O \rightarrow CO_2 + H$	3.0^{-13}	Niki, est.	-98.05
6. $OH + O \rightarrow O_2 + H$	5.0^{-11}	Kaufman(1964)	-16.79
7. $CHO + H \rightarrow CO + H_2$	4.0^{-12}	Niki, et al (1969)	-75.62
8. $OH\dagger_{(v=1)} \rightarrow OH + h\nu$	3.3	Potter, et al (1971)	
9. $CHO + O_2 \rightarrow CO + HO_2$	2×10^{-13}		-18.88
10. $OH\dagger + O \rightarrow O_2 + H$	5.0^{-11}	Kaufman (1964)	
11. $OH + OH \rightarrow H_2O + O$	2.5^{-12}	Dixon-Lewis et al (1966)	-16.95
12. $OH + OH \rightarrow H_2O\dagger + O$	2.5^{-13}	Estimate	
13. $CH_3 + O_2 + M \rightarrow CH_3O_2 + M$	8.0^{-32}	Heicklen	
14. $H + O_2 + M \rightarrow HO_2 + M$	3.0^{-32}	Kaufman (1964)	-47.4
15. $H_2O\dagger + M \rightarrow H_2O + M$	1.0^{-12}	Estimate	
16. $H_2O \rightarrow H_2O + h\nu$	30	Penner (1959)	
17. $HCHO + O \rightarrow CHO + OH$	1.6^{-13}	Niki, et al (1969)	-24.77
18. $CHO + O \rightarrow CO + OH\dagger$		Calculated	
19. $OH + HCHO \rightarrow H_2O\dagger + CHO$	1.4^{-12}	Estimate	
20. $OH + H_2 \rightarrow H_2O + H$	6.6^{-15}	Greiner(1969)	-119.234

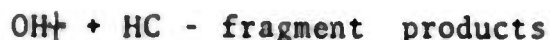|			
21.	$OH + HO_2 \rightarrow H_2O + O_2$	1.0^{-11}	Kaufman (1964) -71.87
22.	$HO_2 + O \rightarrow OH + O_2$	1.0^{-11}	Lloyd (1970) -54.2
23.	$H + HO_2 \rightarrow OH\dagger + OH$	1.0^{-12}	Crutzen (1971) -38.4
24.	$OH + HO_2 \rightarrow H_2O \dagger + O_2$	1.0^{-12}	Estimate
25.	$C_2H_4 + O \rightarrow CH_3 + CHO\dagger$	5.2×10^{-14}	Estimate
26.	$CHO\dagger + O \rightarrow CO + OH\dagger$	1.0^{-11}	Estimate
27.	$H + HO \rightarrow OH + OH$	1.0^{-11}	Estimate
28.	$O + HO_2 \rightarrow OH\dagger + O_2$	1.0^{-12}	Estimates
29.	$CO + OH \rightarrow CO_2 + H$	1.5^{-13}	Wilson (1972)
30.	$OH\dagger + O_2 \rightarrow O_2(b^1\Sigma_g) OH$	3×10^{-14}	Potter, et al
31.	$CH\dagger + H \rightarrow H_2 + O$	1×1.0^{-12}	Estimate
32.	$O_2 (b^1\Sigma) + O_2 \rightarrow O_2 + O_2$	3×10^{-16}	Estimate
33.	$O_2 (b^1\Sigma) + O \rightarrow O_2 + O$	2×10^{-13}	Estimate
34.	$O_2 (b^1\Sigma) + H \rightarrow O_2 + H$	2×10^{-13}	Estimate
35.	$H + HCHO \rightarrow H_2 + CHO$	1×10^{-13}	Westenburg and Dehaas (1972)
36.	$CHO\dagger + O_2 \rightarrow CO + HO_2$	1×10^{-11}	Estimate
37.	$O \rightarrow 1/2\, O_2$	137	Estimate, wall deactivation
38.	$H \rightarrow 1/2\, H_2$	137	Estimate
39.	$OH\dagger \rightarrow OH$	137	Estimate
40.	$H_2O\dagger \rightarrow H_2O$	137	Estimate
41.	$CHO\dagger \rightarrow CHO$	137	Estimate
42.	$O_2 (b^1\Sigma_g) \rightarrow O_2 (X^3\Sigma)$	137	Estimate
43.	Dummy		
44.	$OH\dagger + M \rightarrow OH + M$	1.5×10^{-14}	Estimate
45.	$OH\dagger + H_2 \rightarrow H_2O + H$	1×10^{-14}	Estimate
46.	$C_2H_4 + OH \rightarrow CH_3 + HCHO$	1.8×10^{-12}	Morris & Niki (1971)

In the general case, as in Figure 2, both the OH fundamental and the H_2O ν_3 band could be expected to contribute to emission near 2.7μ. In order to simplify the initial kinetic system, Malki (1972) decided to work at small C_2H_4 concentration in order to minimize the H_2O production. In addition, the O_2 concentration was minimized in order to avoid the reactions

$$H + O_2 + M \rightarrow HO_2 + M \tag{14}$$

$$O + HO_2 \rightarrow OH\dagger + O_2 \tag{29}$$

$$H + HO_2 \rightarrow OH\dagger + OH \tag{24}$$

$$OH + HO_2 \rightarrow H_2O\dagger + O_2 \tag{25}$$

The minimization of the C_2H_4 also prevented significant contributions from

$$OH + C_2H_4 \rightarrow products \tag{47}$$

$$OH + H_2 \rightarrow H_2O\dagger + H,$$
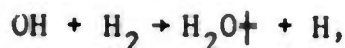
as well as minimizing the contribution of

$$OH\dagger + C_2H_4 \rightarrow products \tag{48}$$

$$OH\dagger + HC - fragment \quad products$$

to the OH loss. Under such circumstances, the major OH loss process will be via

$$OH\dagger + O \rightarrow O_2 + H, \tag{10}$$

which is extremely fast, even for the ground state OH molecule. In fact, reaction with O as a homogeneous loss process is so rapid that OH$\dagger$ deactivation on the wall, which would be diffusion controlled even if every wall collision were effective in de-activation, can be neglected. In the present work the entire range of stoichiometric possibilities were covered in order to test all of the above hypothesis.

15

B. H + NO$_2$

The reaction products for this system have been established
by Kaufman to be NO + OH. Energetically, only two quanta of
vibration can be given to OH in the creation of that new bond.
Kaufman accounted for nearly all of the product in the ground
vibrational state through absorption spectroscopy. We had
previously investigated this reaction via emission spectroscopy
and agreed that the quantum yield for vibrationally excited
OH was very small. A complicating factor is the reaction

$$OH + OH \rightarrow H_2O + O,$$
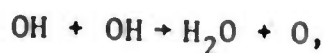
in which the product H$_2$O could also radiate in the 2.7μ region.
Hence, radiometric measurements alone at 2.7μ could not distinguish
between OH and H$_2$O emission, although kinetic considerations would
favor OH. The rate constant for

$$H + NO_2 \rightarrow NO + OH$$
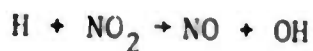
is 4.9 X 10^{-11} cc/sec at 300°K, whereas the rate constant for

$$OH + OH \rightarrow H_2O + O$$
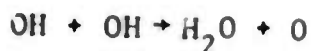
is 2.5 X 10^{-12} cc/sec.

C. $O + C_2H_2$

The product of oxygen atom attack on acetylene has been
established by Kanofsky, et al (1972) and by Jones and Bayes (1972)
to be

$$O + C_2H_2 \rightarrow CH_2CO \qquad 25\%$$
$$CH_2 + CO \qquad 15 - 45\% \left.\right] 75\%$$
$$HCCO + H \qquad 30 - 60\%$$
$$C_2O + H_2 \qquad .3\%$$

with HCCO being rapidly consumed by O atoms to give

$$HCCO + O \rightarrow H + 2CO$$

Thus, CO is a major species formed by very exothermic reactions
so that highly vibrationally excited CO is expected from his
system, but little or no OH or H_2O is expected.

D. $H + HO_2$

The reaction

$$H + HO_2 \rightarrow 2OH\dagger$$
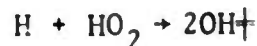
has been studied by Charters and Polanyi, (1960). Those authors
concluded that this very rapid reaction produces vibrationally
excited OH†.

INFRARED SPECTOSCOPY: RESULTS AND DISCUSSION

In order to establish the mechanism for O atom attack on reactive hydrocarbons and thereby quantify and interpret filter-kinetic data, in both the visible and infrared, we have taken extensive spectral measurements in the 1-3μ region, using a Jarrel Ash quarter meter monochrometer and an ITO Pbs detector. The total pressure for these measurements was about 1000 - 1200μ.

The wavelength calibration for this region was achieved using the CO first overtone generated by the reaction of $O + C_2H_2$ illustrated in Figure 3. For most of the spectra, the resolution was better than 0.03μ so that the location of the maxima between 2.33 and 2.61 provides an excellent calibration.

For the oxygen atom attack on ethylene, three prominent features are observed. The first is near 1.4 - 1.5μ which could be H_2O, OH first overtone, or CO second overtone. The second feature appears near 2.3μ which could be the CO first overtone observed in Figure 3 for the $O + C_2H_2$ system. The third feature occurs near 2.7μ and could be either the H_2O ν_3 band or the OH fundamental. Precise identification of the emitting species from the spectra alone is difficult because of several reasons. First the system is highly non-equilibrium in nature with the vibrational temperature of the emitting species far exceeding the rotational and kinetic temperatures. Thus equilibrium spectra cannot be used for easy comparison. Second, the overlapping of spectra from two or more species which is certainly expected in the case of OH and H_2O does not permit unique identification of band shapes. Third,

Figure 3. The first overtone of CO generated by reaction of O atoms with C_2H_2 in a fuel rich system at 1 torr total pressure using a Jarrel Ash quarter meter monochronator with 1000μ slits.

1000$_\mu$ SLITS, 100$_\mu \nu$ F.S., τ=3, 2/5 RPM MOTOR, 2 MIN/IN, 71$_\mu$ C_2H_2, 16μ O, 808$_\mu$ He, 200$_\mu$ O_2 1st WINDOW.

CO OVERTONE
$O+C_2H_2$

WAVELENGTH, μ

2.3　2.5　2.7

Figure 3.

20
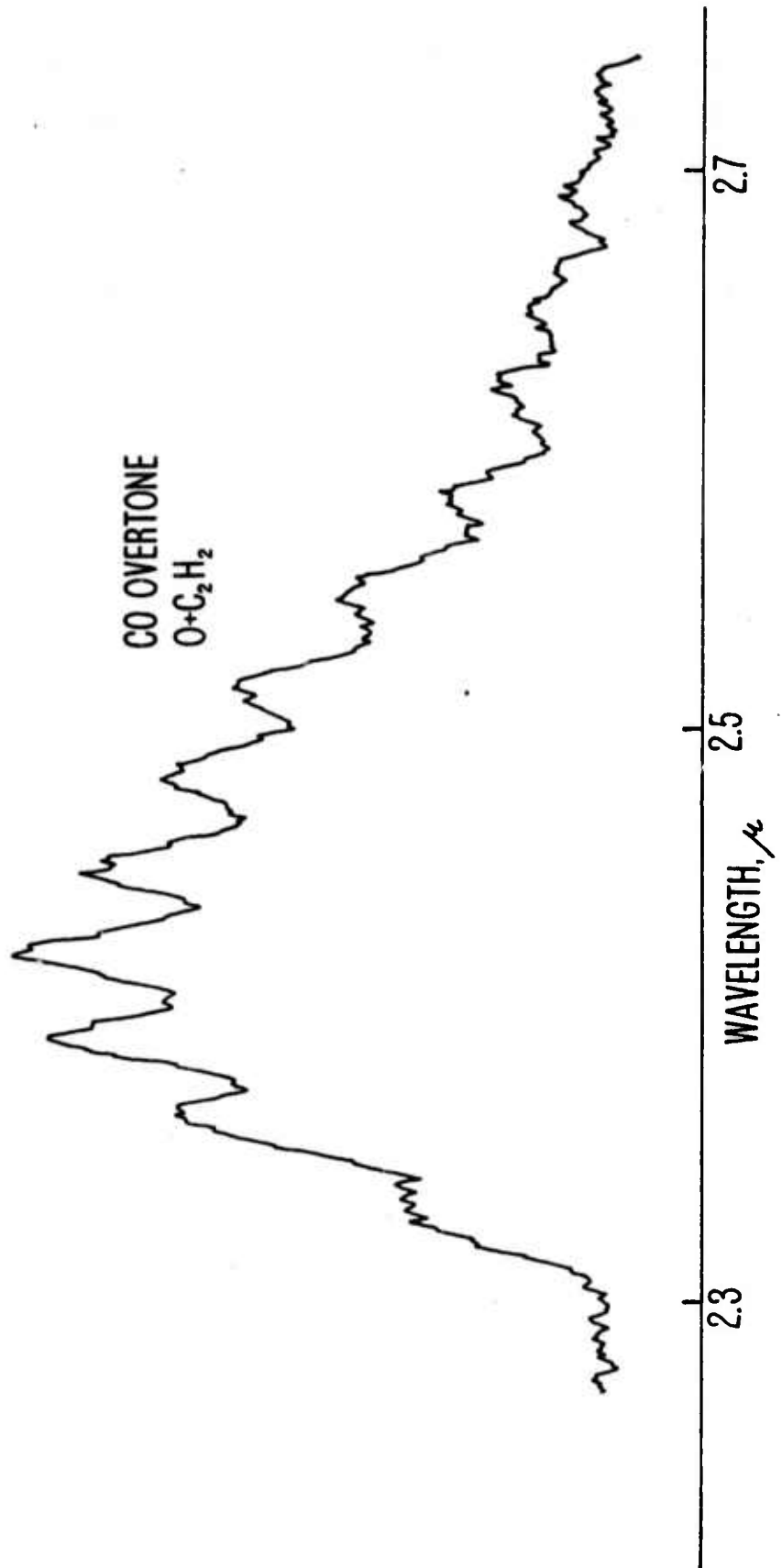
the relatively low resolution spectra do not permit exact location of individual line positions. Therefore, in addition to the spectra themselves, we have employed the kinetic arguments previously discussed in order to plan and interpret changes in the spectra as a function concentration and additives.

First, we expect that the spectrum in a large excess of O atoms and for small concentrations of HC ($<1\mu$ Malki, 1972) should show a predominance of OH emission over H_2O emission, at least for short contact times. In addition, CO emission should also be predominant under these conditions (low HC, short contact times) since CO is a direct product of the reaction which produces OH :

$$CHO + O \rightarrow CO + OH.$$
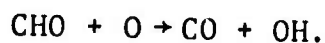
It is presumably unlikely that CO is a new bond in this reaction and thus we initially did not expect to see the CO first overtone from ethylene oxygen atoms unlike the acetylene plus oxygen atom case. Water is produced by a subsequent reaction of OH with another hydrocarbon fragment. Hence H_2O emission should be quadratically dependent on the hydrocarbon concentration.

To test these ideas, we examined the spectra from very small concentrations ($<1\mu$) to nearly 100μ of ethylene. In Figure 4, we illustrate spectra taken at constant resolution and a constant contact time of about three milliseconds over an ethylene concentration range of 2μ to 85μ . As illustrated in Figure 4, the 2.7μ peak predominates over the 2.3μ peak at low concentrations but the reverse is true at high concentrations. In addition, there are two features at 2.3μ which also undergo an intensity reversal. Clearly, a quadratic dependence of the intensity is not observed.

Figure 4. The near infrared emission spectrum generated by the reaction of O atoms with ethylene for various concentrations of ethylene at a contact time of less than 2 msec and an oxygen atom concentration of approximately 10μ.

STARTING FROM BOTTOM CURVES:

$2_\mu C_2 H_4$ (1) 1000_μ SPLITS, 20_μ ν F.S., 10_μ F.S., $\tau=10$, 5 min/in, 1 RPM, $200_\mu O_2$, 800_μ He $\sim 11_\mu$ O., 1st WINDOW

$3_\mu C_2 H_4$ (2) 1000_μ SLITS, $20_\mu \nu$ F.S., 10_μ F.S., $\tau=10$, 5 min/in, 1 RPM 200_μ O_2 800_μ He, $\sim 11_\mu$ O., 1st WINDOW

$10_\mu C_2 H_4$ (3) 1000_μ SLITS, $50_\mu \nu$ F.S., 100_μ F.S., $\tau=10$, 5 min/in, 1 RPM 800_μ He $200_\mu O_2$, 11_μ O, 1st WINDOW

$45_\mu C_2 H_4$ (4) 1000_μ SLITS, $50_\mu \nu$ F.S., 100_μ F.S., $\tau=10$, 5 min/in, 1 RPM 800_μ He $200_\mu O_2$, 11_μ O, 1st WINDOW

$85_\mu C_2 H_4$ (5) 1000_μ SLITS, 50_μ ν F.S., 100_μ F.S., $\tau=10$, 5 min/in, 1 RPM 800_μ He $200_\mu O_2$, 11_μ O, 1st WINDOW

50 μv
GAIN
85 μ ETHYLENE

50 μv
45 μ

50 μv
10 μ

20 μv
3 μ

20 μv
2 μ

1.0   2.0   3.0
WAVELENGTH, μ
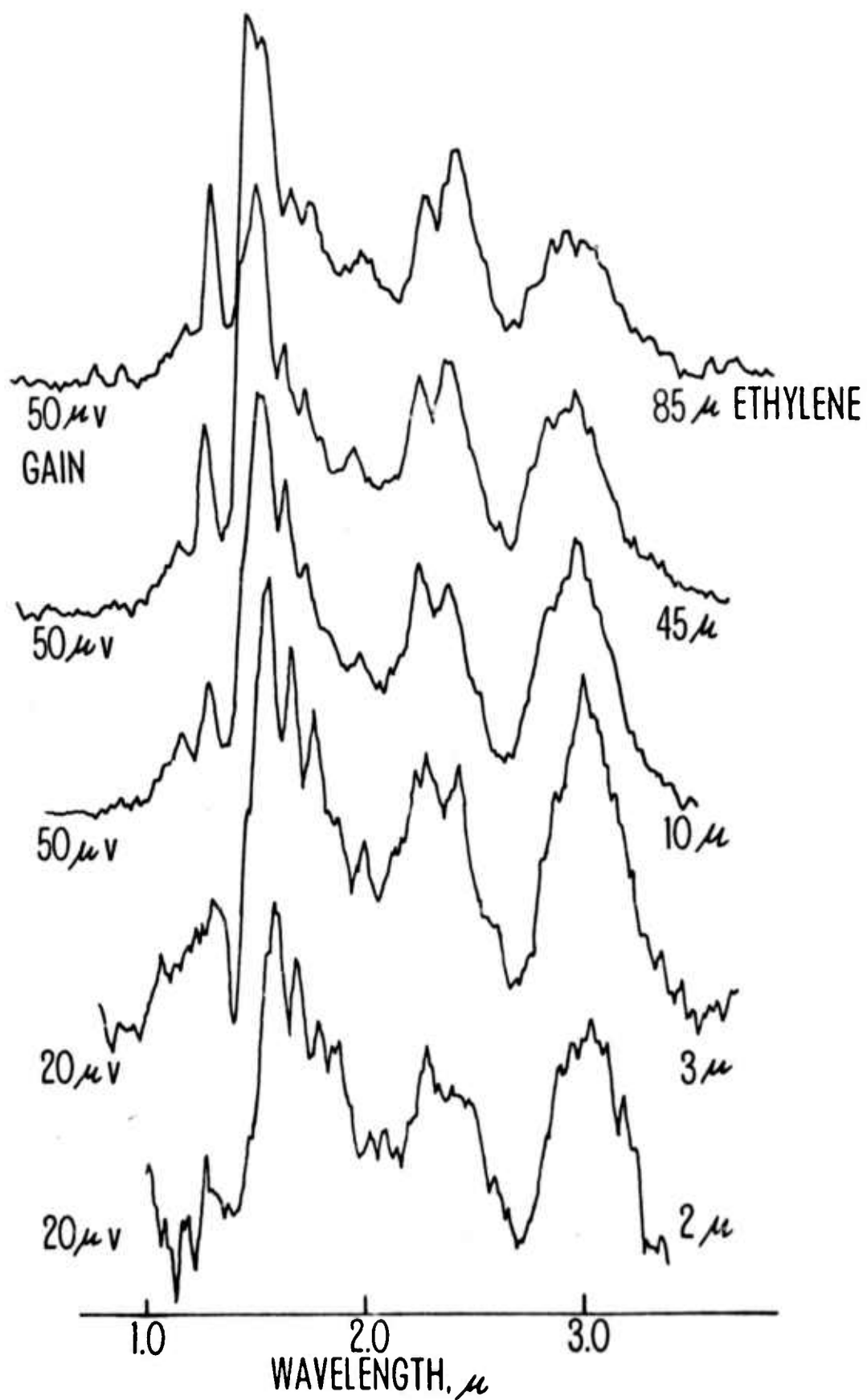
Figure 4.   23

The feature at 2.7μ is very similar to the observed OH
intensity from the reaction

$$H + O_3 \rightarrow OH\dagger + O_2$$

obtained by Murphy (1971), illustrated in Figure 5. That
reaction is 77 Kcal exothermic. The reaction of CHO + O is even
more exothermic and hence many overlapping transitions from OH
$\Delta v = 1$ are possible in both cases. A cleaner spectrum of OH
in which a maximum of two vibrational quanta can be excited
can be obtained from the reaction

$$H + NO_2 \rightarrow NO + OH\dagger$$
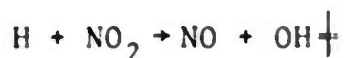
At concentrations of NO_2 sufficiently low, the primary step occurs
in a few milliseconds, while the recombination of OH to yield
water requires tens of milliseconds, presumably via the reaction

$$OH\dagger + OH \rightarrow H_2O + O.$$
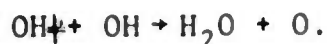
In Figures 6 and 7 we illustrate the spectrum for $O + C_2H_4$ and
the spectrum for $H + NO_2$ taken at (H) $\approx$ (NO_2) $\approx$ 4.5. Two
overlapping $\Delta v = 1$ transitions are possible at 2.7μ, but only
one $\Delta v = 2$ transition, with a resulting narrower peak is possible
at $1.4 - 1.5\mu$. Again in this system, a quadratic dependence of
the intensity of H_2O emission on NO_2 concentration would be
expected and our kinetic studies do not show this. In any event
no peak at the 2.3μ region occurs in the $H + NO_2$ system and
therefore we conclude that the 2.3μ peak is no OH emission, but
rather CO first overtone emission. Using the NO + O calibration, we
find that the ratio of the 1.5μ intensity to the 2.7μ intensity is
0.447 compared to the value of $0.44 \pm .03$ determined by Murphy (1971)
for the OH overtone to fundamental intensity ratio.

Figure 5. The emission spectrum in the fundamental and first overtone of OH due to the reaction $H + O_3$ from Murphy, (1971).
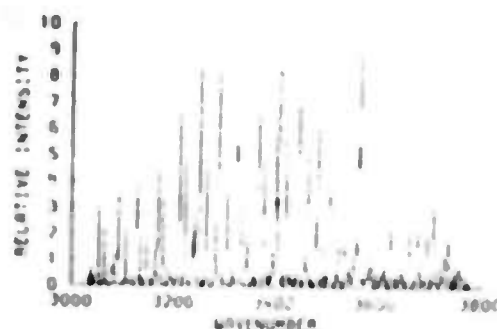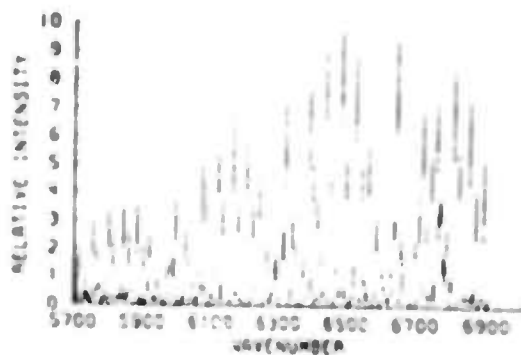
Figure 2. A comparison of the infrared emission spectra for the reactions $O + N_2H_4$, $O + C_2H_4$ and $H + NO_2$. Concentrations of O and H were approximately 10μ and the concentrations of N_2H_4, C_2H_4 and NO_2 were approximately 2μ, 10μ, and 4.5μ respectively. All spectra were taken at a contact time of less than 2 msec. Both O and H were diluted in a stream consisting primarily of He.

$H + NO_2 \rightarrow$; 2000μ slits, $50\mu vFS$, $100\mu FS$, $\tau = 10$, 1 RPM, 5 Min/in, $800\mu He$, $200\mu H_2$, $5\mu NO_2$, 5μ 1st WINDOW.

$O + C_2H_4 \rightarrow$; 1000μ slits, $50\mu vFS$, $100\mu FS$, $\tau = 10$, 1 RPM, 5 Min/in, $10\mu C_2H_4$, $800\mu He$, $200\mu O_2$, $11\mu O$ 1st WINDOW.

$O + N_2H_4 \rightarrow$; 2000μ slits, $20\mu vfs$, $100\mu FS$, $\tau = 3$, 2 Min/in, 4 RPM, $2\mu N_2H_4$, $900\mu He$, $90\mu O_2$; $11\mu O$; 1st WINDOW.
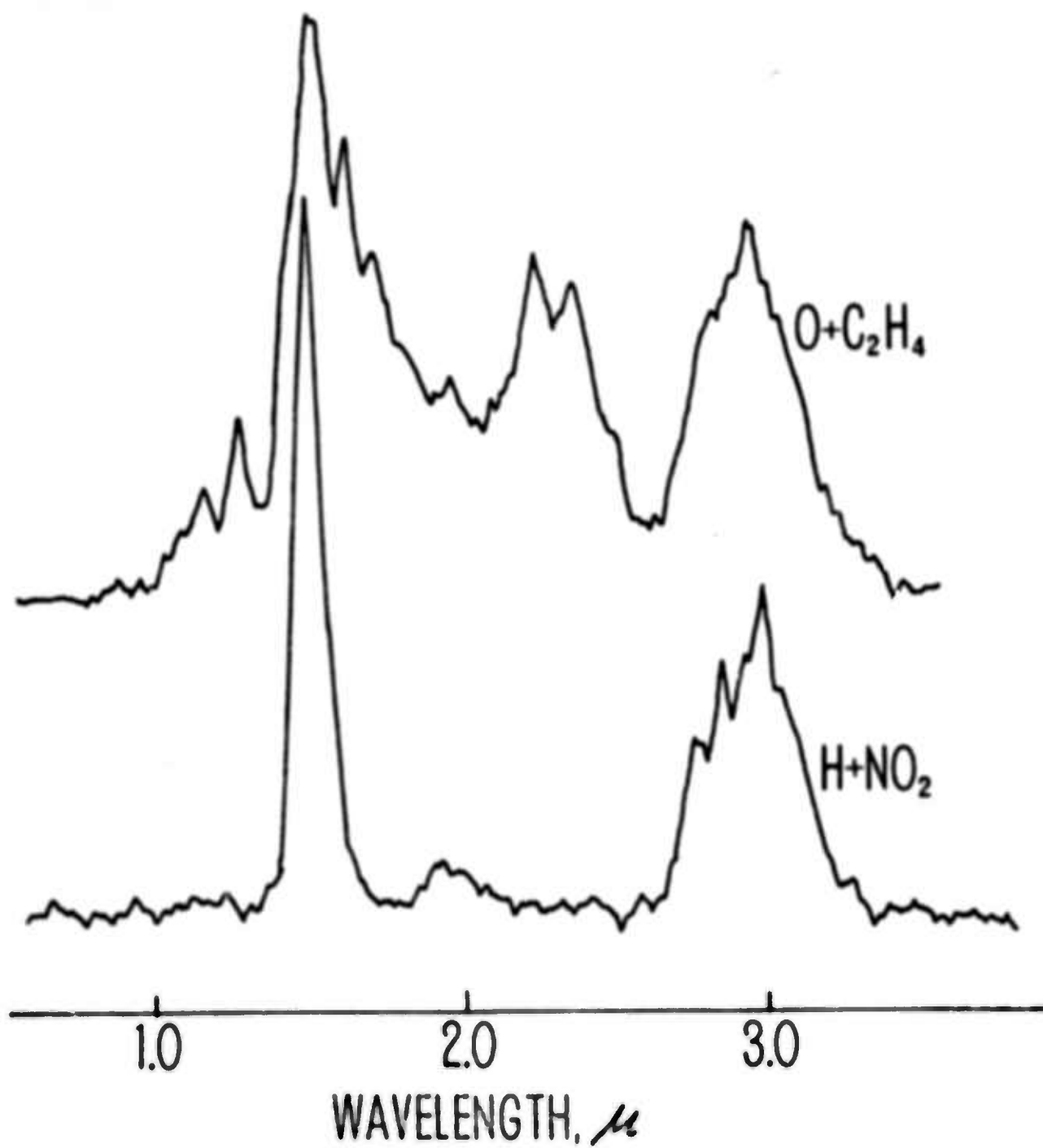
Figure 6.

Figure 7. A comparison of the infrared emission spectrum of $0 + C_2H_4$ and $H + NO_2$. Conditions are similar to those of Figure 6 except that pure oxygen was discharged to obtain 0 atoms and no He was added. Hence a great excess of 0_2 exists in this system.

$H + NO_2 \rightarrow$: $4.5_\mu NO_2$, $200_\mu H_2$, $800_\mu He$, $4_\mu H_2$ 2000_μ slits, $100_\mu FS$, $20_\mu vFS$, 1 RPM $\frac{2 \text{ Min}}{\text{in}}$, $\tau = 10$, 1st WINDOW.

$0 + C_2H_4 \rightarrow$: 2000_μ slits, $630_\mu 0_2$, $4.5_\mu C_2H_4$ $100_\mu FS$, $100_\mu vFS$, $\tau = 3$, 1 RPM, $\frac{2 \text{ Min}}{\text{in}}$, 1st WINDOW.

An additional test for these tentative identifications might be achieved by adding a reactant which preferentially eliminates one of the possible radiators by reaction or energy transfer. One candidate is CO, which undergoes a moderately fast reaction with OH but is not expected to alter H_2O emission. Energy transfer by excited CO to added "cool" CO might also be expected to alter the CO intensity distribution. This effect is readily observed by addition of CO to the oxygen atom plus acetylene system in Figure 8, where 290μ of CO is added to the reaction mixtures. The total intensity of the CO first overtone is greatly reduced and the distribution is altered slightly. As illustrated in Figure 9, an even more pronounced effect occurs at the 2.3μ peak in the $O + C_2H_4$ spectrum at the same CO concentration. At this concentration of CO, little effect on the peaks at 1.4 and 2.7μ was observed. With a rate constant of 1.5×10^{-13} cc/sec for the reaction

$$CO + OH \rightarrow CO_2 + H$$

we would expect an effective first order rate constant of

$$1.5 \times 10^{-13} = 1.5 \times 10^3,$$

for the loss mechanism of OH via this reaction. This must be compared to the other loss mechanism for OH^+,

$$OH^+ + O \rightarrow O_2 + H,$$

which has a rate constant of approximately 4×10^{-11} cc/sec. Hence, with an oxygen atom concentration of approximately 3×10^{14}/cc the dominant OH loss mechanism remains O atom attack, with an effective first order rate constant of 1.2×10^4.

In the case of the $H + NO_2$ system, where OH^+ loss is
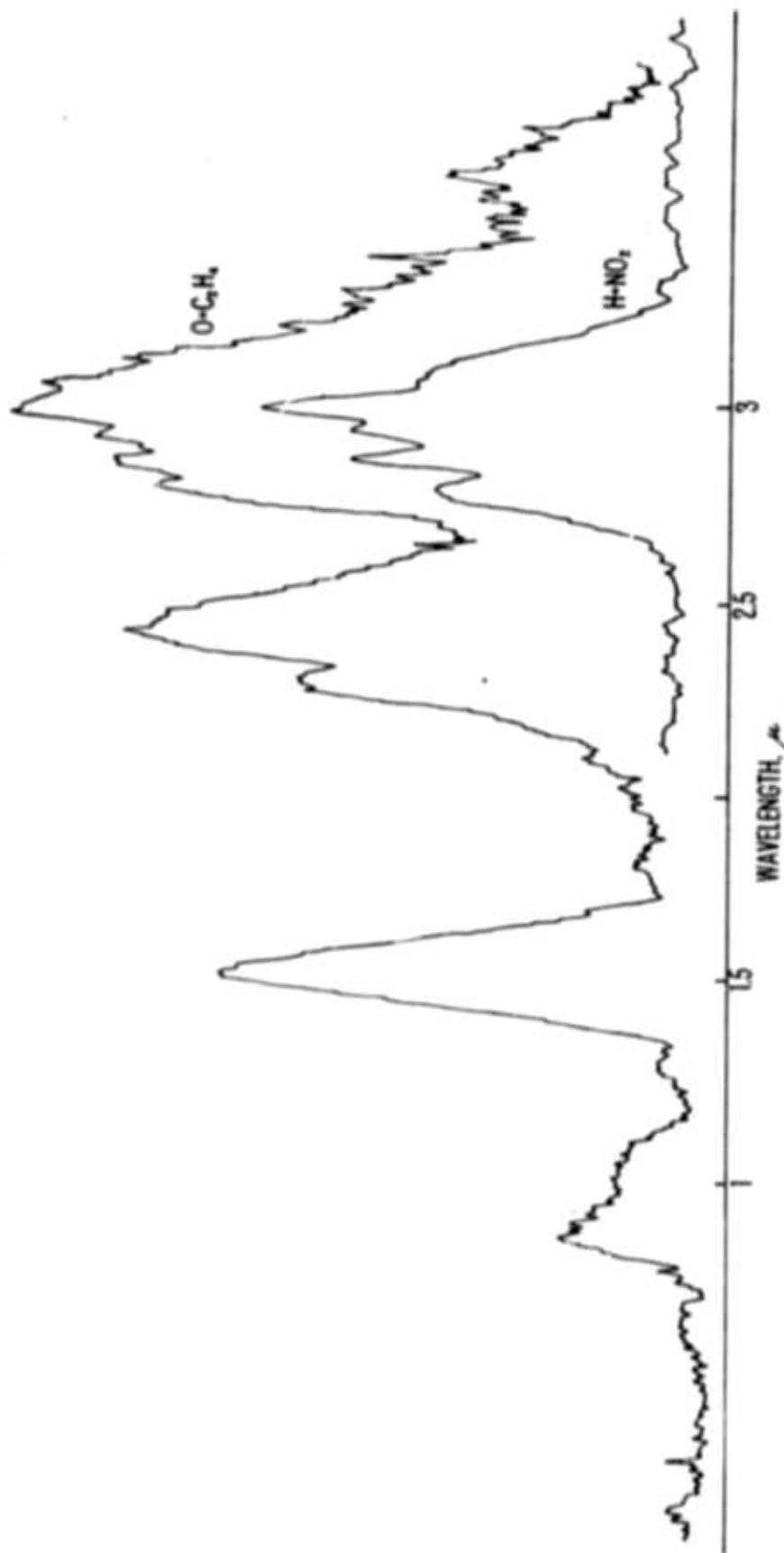
Figure 7.

Figure 8.   The effect of an addition of 150µ of CO to the

0 → C_2H_2 system.

Conditions for both: 1000_μslits, $\frac{2}{5}$ RPM, $\frac{5 \text{ Min}}{\text{in}}$, $\tau = 10$,

50_μvFS $59_\mu C_2H_2$, $208_\mu O_2$, 812_μHe, $\sim 8_\mu$0 270_μ Ar.

C₂H₂+O →
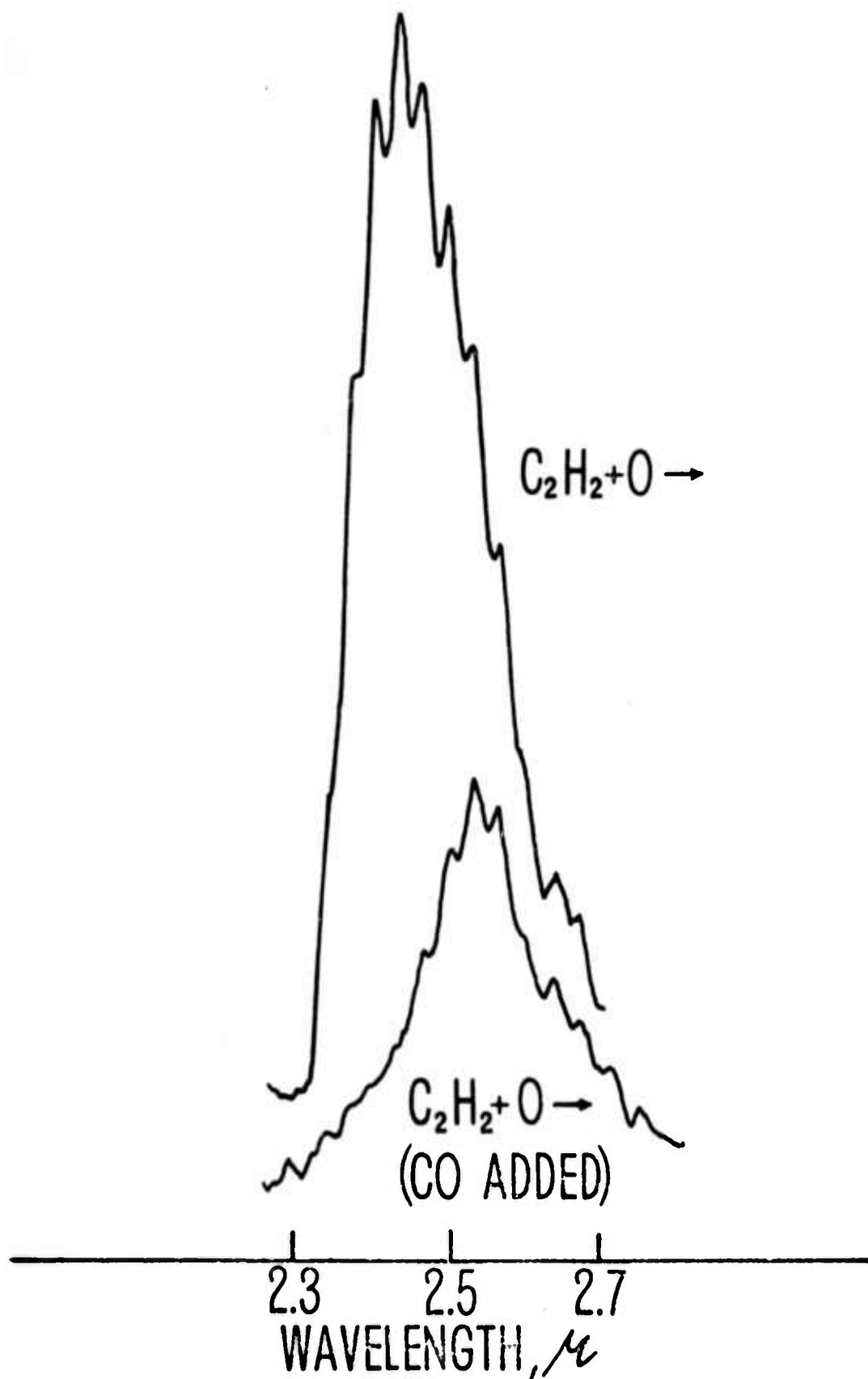
C₂H₂+O →
(CO ADDED)

2.3   2.5   2.7

WAVELENGTH, μ

Figure 8.

32

Figure 9. The effect of additives on the $0 + C_2H_4$ emission spectrum. $240_\mu CO_2$ and $236_\mu CO$ were added.

Conditions for all: 1000_μslits, 1 RPM, $\frac{5\ Min}{in}$, $\tau = 10$, $50_\mu vFS$, $100_\mu FS$, $50_\mu C_2H_4$, $208_\mu O_2$ $812_\mu He$, $8_\mu 0$, 1st (KB_r) WINDOW.

O+C₂H₄

O+C₂H₄

(CO₂ ADDED)

O+C₂H₄

(CO ADDED)

WAVELENGTH, μ

Figure 9.

34

presumably via

$$OH\dagger + OH \rightarrow H_2O + O,$$
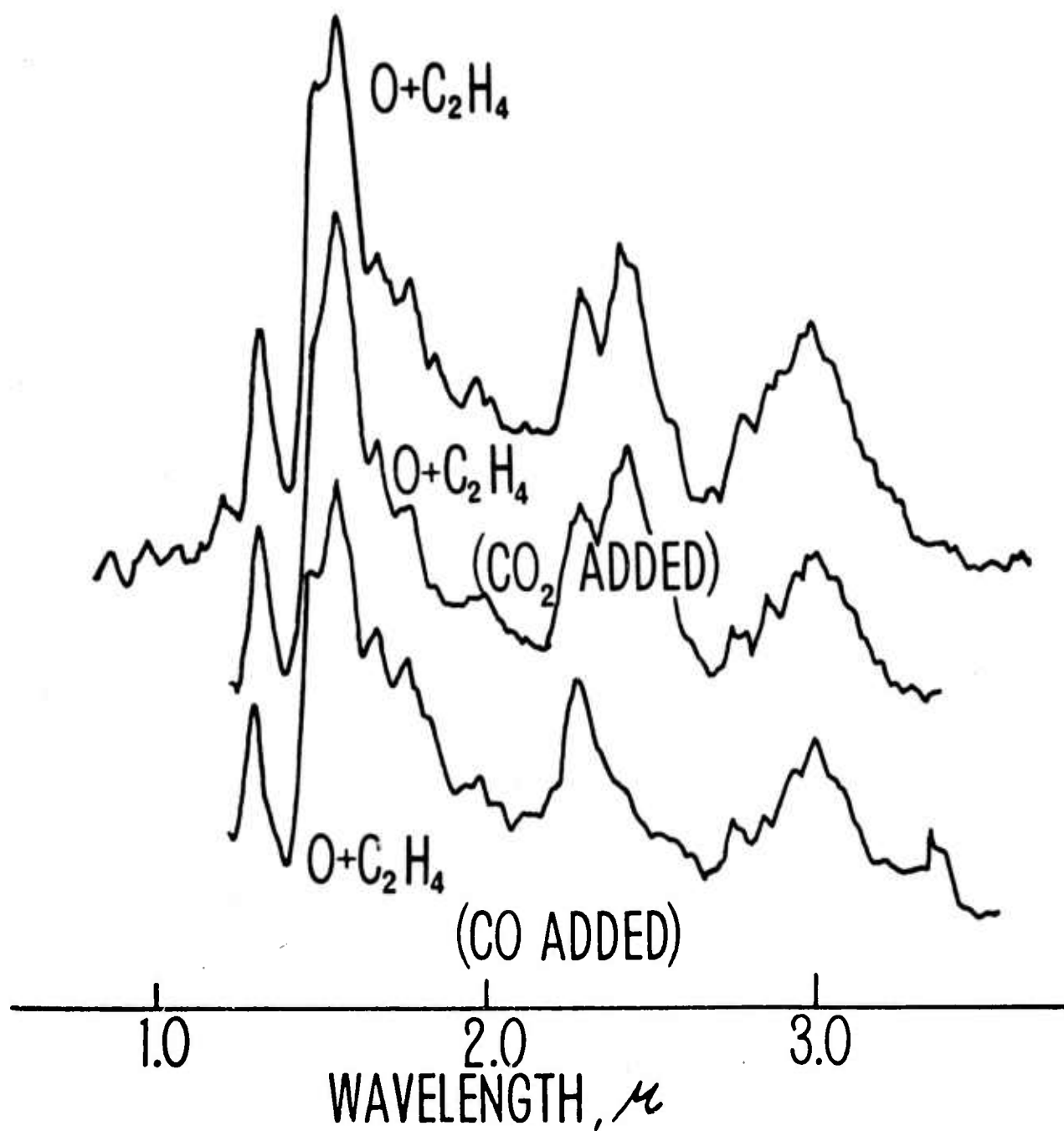
a much slower reaction, it should be possible to attenuate the
OH signal via CO scavenging. As shown in Figure 10 this indeed
does happen. In addition, other species which react with OH
have been added to this system. In general, we see from Figure 10
that the more rapid the reaction with OH, the smaller the signal
in both the OH fundamental and the OH overtone. The overtone
decreases more rapidly than the fundamental, which is con-
sistent with the narrowing of the fundamental band also observed.

Thus, we conclude on the basis of kinetic arguments as
well as spectral arguments that the observed emission at
2.7µ is due to the OH fundamental and the emission at 1.5µ
is the OH overtone.

As shown in Figure 11, we also observe these features in
the $H + HO_2$ system; however, the conditions necessary to achieve
this signal level in Figure 11 make it impossible to permit
$H + HO_2$ to be the cause of the OH emission in the $O + C_2H_4$
system.

In summary, we present in Figure 12, a compilation of
infrared signatures at a contact time of 2 msec due to O atom
attack on various hydrocarbons.

Figure 10. The effect of additives on the H+NO$_2$ infrared emission signal.

Conditions Common to All: 2000$_\mu$slits, $\frac{5 \text{ min}}{\text{in}}$, 1 RPM, 774$_\mu$He, 222$_\mu$ H$_2$, 5$_\mu$NO$_2$ 1st WINDOW, τ=10, 100$_\mu$ vF.S.

Starting from Top:

NO$_2$+H → (Ar): 1 Torr Ar, 1 Torr F.S.

NO$_2$+H → (CO): 780$_\mu$CO, 1 Torr F.S.

NO$_2$+H → (C$_2$H$_2$): 310$_\mu$C$_2$H$_2$, 1 Torr F.S.

NO$_2$+H → (C$_2$H$_6$): 0.5 Torr C$_2$H$_6$, 1 Torr F.S.

NO$_2$+H → (n-C$_4$H$_{10}$): 370$_\mu$n-C$_4$H$_{10}$, 1 Torr F.S.

NO$_2$+H → (C$_3$H$_6$): 345$_\mu$C$_3$H$_6$, 1 Torr F.S.
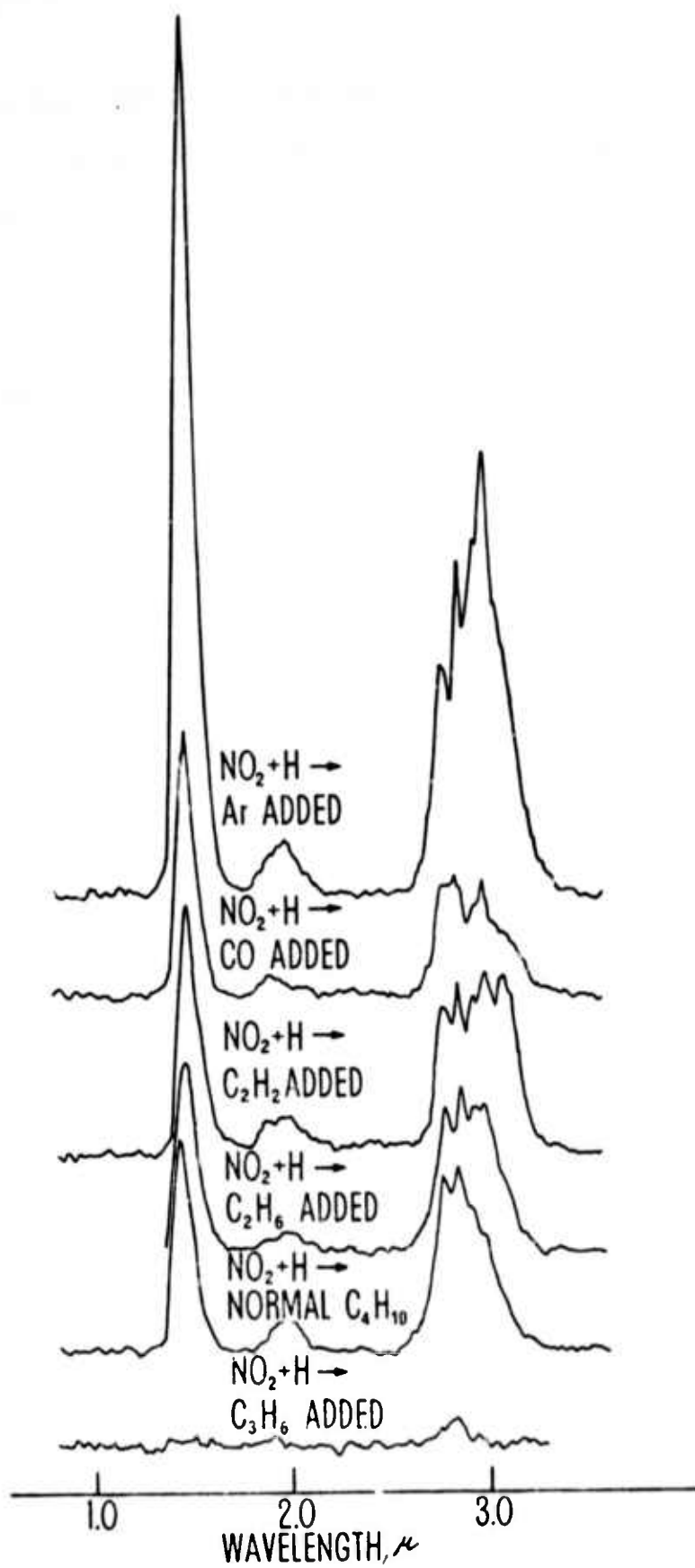
Figure 10.

Figure 11. A comparison between the $H+NO_2$ and $H+HO_2$ infrared emission signals. Exactly 3200_μ O_2 was added to the H_2 in He discharge in order to observe the $H+HO_2$ signal at a contact time of 2 msec.

Conditions for Both: 2000_μ Slits, $\tau=10$, 1st WINDOW 100_μ F.S., 100_μ v F.S., IRPM, $\dfrac{5 \text{ min}}{\text{in}}$, $222_\mu H_2$, 774_μ He., $5_\mu NO_2$.
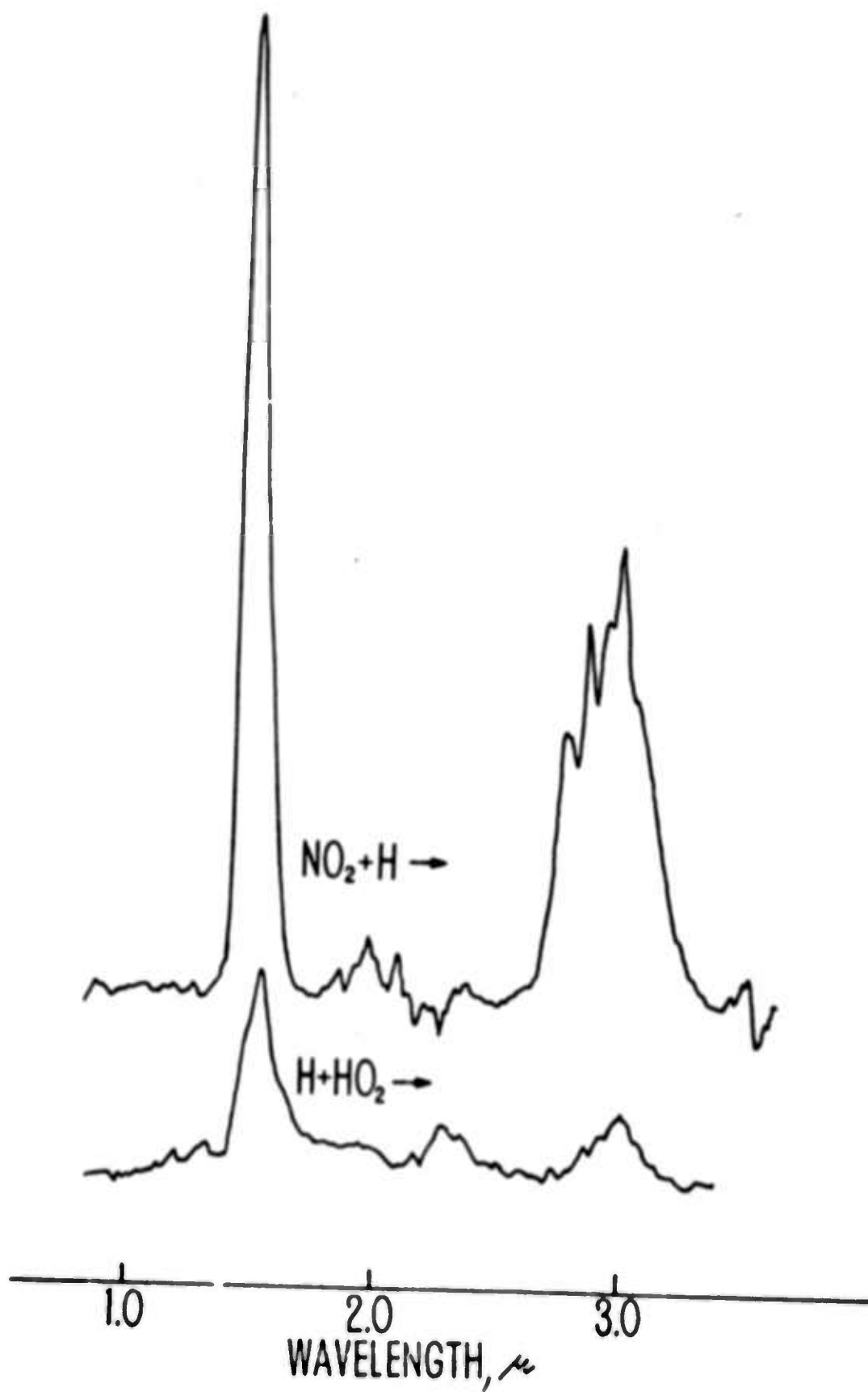
Figure 11.

Figure 12. A Summary of infrared signatures initiated by O atom attack on selected hydrocarbons.

Conditions for All: 1000_μ Slits, IRPM $\frac{5 \text{ min}}{\text{in}}$, $\tau=10$ 50_μ vF.S., 100_μ F.S., 1st WINDOW, 774_μ He $195_\mu O_2$, 250_μ Ar.

Starting from Top:

$C_2H_2 + O \rightarrow$: $53_\mu C_2H_2$

$C_2H_4 + O \rightarrow$: $55_\mu C_2H_4$

$C_3H_6 + O \rightarrow$: $70_\mu C_3H_6$

$n-C_nH_{10} + O \rightarrow$: $62_\mu n-C_4H_{10}$

$C_2H_6 + O \rightarrow$: $36_\mu C_2H_6$
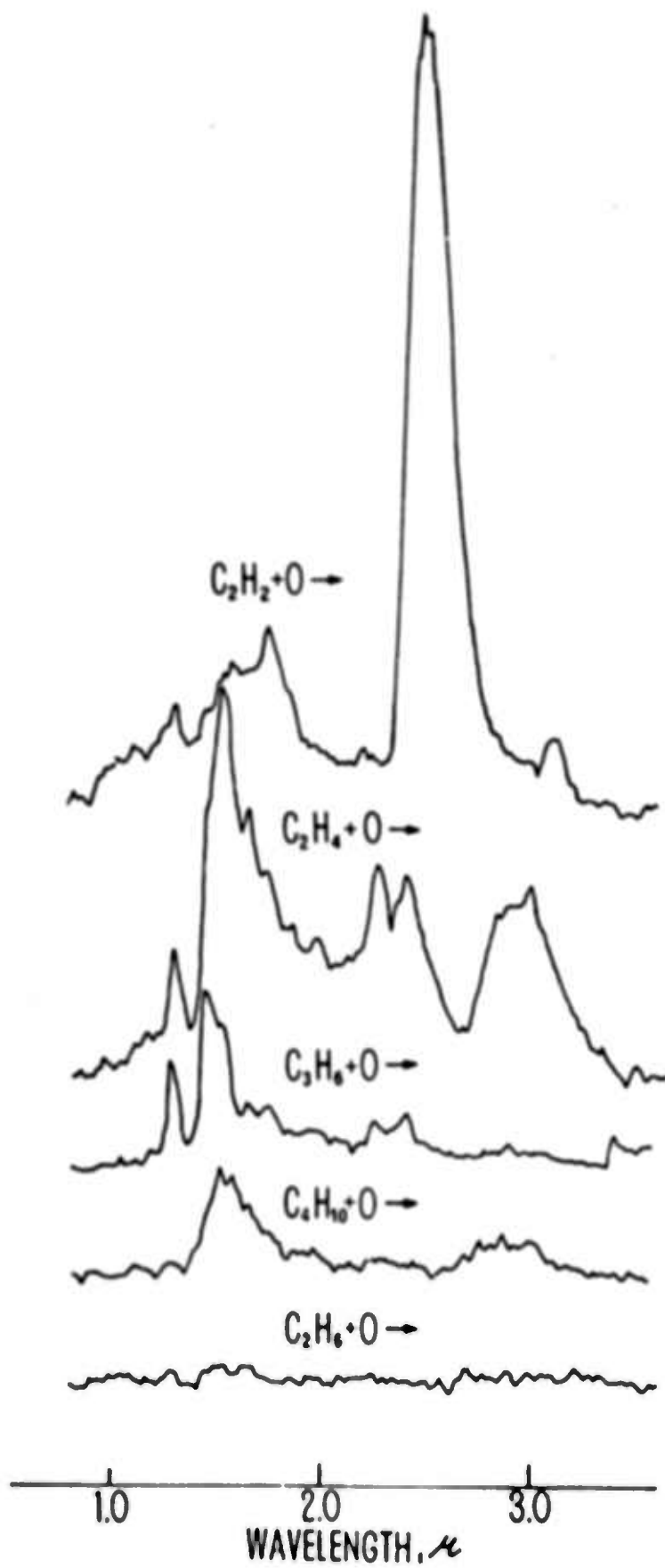
Figure 12.

ACKNOWLEDGMENTS

REFERENCES

Atkinson, R., and R. Cvetanovic, J. Chem. Phys. 56, 432 (1972).

Baulch, D., D. Drysdale, and A. Lloyd, Leeds Report Nos. 1-4.
1968.

Browne,W., R. Porter, J. Verlin, and A. Clark, Twelfth Symp.
(Int.) on Combustion, the Combustion Institute, Pittsburgh,
Pennsylvania, 1035 (1969).

Charters, P., and J. Polanyi, Canadian J. Chem. 38, 1742 (1960).

Clyne, M.,m Ninth Symp. (Int.) on Combustion the Combustion
Institute, Pittsburgh, Pennslyvania, 211 (1963).

Davis, D., R. Huie, J. Herron, M. Kuryld, and W. Braun, J. Chem.
Phys. 56, 4868 (1972).

Dixon-Lewis, G., Wilson, W.E., and A. Westenberg, J. Chem. Phys.
44, 2877 (1966).

Fontijn, A., C. Meyer, and H. Schiff, J. Chem. Phys. 40, 64 (1964).

Herron, J., and R. Penzhorn, J. Phys. Chem. 73, 191 (1969).

Hushafar, F., J. Rodgers, and A.T. Stair, Jr., Applied Optics
10, 1843 (1971).

Jonathan, N., Melliar-Smoth, and D. Salter, Mol. Phys. 20, 93
(1971).

Kanofsky, J., D. Lucas, and D. Gutman, Fourteenth Symposium (Int.)
on Combustion, preprint, 1972.

Kaufman, F., Ann. Geophys. 20, 106 (1964).

Kaufman, F., private communication, 1973.

Krieger, B.,M.Malki, and R. Kummler, Enviromental Science
and Technology 6, to be published (1972).

Krieger, B., and R. Kummler, paper 42b, presented at the 74th
National AIChE Meeting, New Orleans, March 1973.

Kummler, R., E. Fisher, and M. Malki, presented at the DAMP
meeting, University of Windsor, Windsor, Ontario, Canada
April, 1973.

Lloyd, A., NBS Report 10447 (1970).

Malki, M., 'Infrared Chemiluminescence from Oxygen Atom Attack

on Ethylene," Masters Thesis, Wayne State Univesity, December, 1972.

McGrath, W., and R. Norrish, Proc. Roy. Soc. (London) A242, 265,(1957).

Morris and Niki, private communication, 1971.

Murphy, R. J. Chem. Phys. 54, 4852(1971).

Niki, H., E. Daby, and B. Weinstock, Twelfth Symp. (Int.) on Combustion
The Combustion Institute, Pittsburgh, Pennsylvania, 277 (1969).

Pacey, P. and J.C. Polanyi, Appl. Opt. 10, 1725 (1971).

Parker, J., and G. Pimentel, J. Chem.Phys. 51, 91 (1969).

Potter, A., Jr., R.N. Cotharp, and S. Worley, J. Chem. Phys. 54
992 (1970).

Penner, S., "Quantitative Molecular Spectroscopy and Gas Emissions"
Addison Wesley, Reading,Mass. (1959).

Smith, I., to be published, 1972.

Stair, A.T.,Jr., J. Kennealy, S. Stewart, Planet. Space Sci. 13, 1005
(1972).

Stair, A.T.,Jr., and J. Kennealy, J. Chem. Phys. 124 (1967).

Stuhl, F., and H. Niki, J. Chem. Phys. 55, 3954 (1971).

Worley, S., R. Coltharp, and A. Potter, Jr., J. Phys. Chem. 76,
1511 (1972).

THEORETICAL DETERMINATION OF VIBRATIONAL EXCITATION OF MOLECULES

The theoretical program at RIES has been primarily concerned with the calculation of cross sections for the vibrational excitation of molecules by heavy body collisions. This is carried out using a numerical close coupling solution of the wave equation for the colliding system based on the breathing sphere model of Schwartz, Slawsky and Herzfeld (1954) to represent the target molecular vibrator, and an empirical spherically symmetric scattering potential.

Many reactions of interest in the upper atmosphere involve collisions between molecules and atomic oxygen. However, except for a semi-empirical estimate of the $CO-O(^1D)$ interaction (Marriott, 1970) the central potentials necessary for the calculation of these excitation cross sections have not been available until recently.

As detailed in Part III of this report, potentials of the form

$$V(r) = A\exp(-Br)$$

have now been determined experimentally for a number of collision systems of interest. The parametric values required by the collision code are shown in Table 1.

Up to the present time, using this data excitation cross sections have been calculated for the $CO-O(^3P)$ and $N_2-O(^3P)$ systems. Preliminary results based on the coupling of three

molecular vibrational states are shown in Table 2, together with the CO-CO and CO-O(^{1}D) values for comparison.

Although no direct cross section measurements are available for checking these theoretical results, experimental determinations of certain rate coefficients are available (center-1973) and these can in turn be calculated using the cross sections. Thus an indirect comparison with experiment can be obtained and this calculation is presently underway.

In addition to the above, the previous report outlined a recent extension of the original vibration-translation collision code to include vibration-vibration exchange processes. The need for further extension to include virtual states was established if the code was to continue to be able to calculate cross sections at collision energies of interest (i.e.: below 1-2 eV).

The code has now been reconstructed to allow for the occurrence of these virtual states. At this time the new subroutines are being debugged.

Our present plans for future work include the following:

(a) Complete the debugging of the new v-v code including the effects of virtual states.

(b) Complete the vibrational excitation cross section calculations for all the collision systems for which O-molecule scattering potentials are now available (Table 1).

(c) Apply the full code initially to a detailed study of vibrationa. excitation rpocesses in CO, including the effects of vibration-vibration exchange and virtual states. The results will be analysed in comparison with previous theory and experiment to estimate the "physical" reliability of the overall calculation.

Table 1. Experimental central potential parameters for the interaction $V(r) = A\exp(-Br)$ for various $O(^3P)$-molecule collisions.

System	A (atomic units)	B (a_0^{-1})	Expt. range (eV)
$O - CO$	30.77	1.7447	13.6 - 0.4
$O - N_2$	20.92	1.6108	14.8 - 0.4
$O - NO$	38.13	1.7717	13.4 - 0.4
$O - H_2$	18.38	2.1474	14.9 - 0.4
$O - O_2$	62.43	1.9151	12.4 - 0.4
$O - CO_2$	75.55	1.7214	12.4 - 0.4
$O - H_2O$	52.02	1.9579	12.9 - 0.4

Table 2. Calculated cross sections for the vibrational excitation of N_2 and CO assuming coupling between the first three vibrational levels.

Collision system:	$N_2 - O(^3P)$	$CO - O(^3P)$	$CO - CO$[†]	$CO - O(^1D)$[††]
Coll. energy (eV)	$Q_{01}(\pi a_0^2)$	$Q_{01}(\pi a_0^2)$	$Q_{01}(\pi a_0^2)$	$Q_{01}(\pi a_0^2)$
0.266		0.000		
0.292	0.000	----------	0.000	0.000
0.6	----------	----------	----------	0.117(+2) **
0.8	0.578(-8)	0.410(-6)	----------	----------
0.85	----------	----------	0.56(-4)	0.110(+2)
1.0	0.178(-5)	0.680(-5)	----------	0.101(+2)
1.5	0.214(-4)	0.339(-3)	----------	0.85 (+1)
2.0	0.277(-3)	0.265(-2)	0.12(-1)	0.70 (+1)
2.5	----------	----------	0.22	0.60 (+1)

**Figure in brackets shows power of ten by which number must be multiplied.

†Marriott & Gianturco (1970)

††Marriott (1970)

References

R. Center, experimental work detailed in AVCO Semi-Annual Reports to ARPA Plume Physics Program (1973).

R. Marriott, Research Institute for Engineering Sciences Report-RIES 70-17, November (1970).

R. Marriott and F. A. Gianturco, J. Phys. $\underline{B2}$, 1332 (1969).

R. N. Schwartz, Z. I. Slawsky and K. F. Herzfeld, J. Chem. Phys. $\underline{20}$, 10 (1951).

PART III: Determination of the Intermolecular Potentials

between Oxygen Atoms and Plume Species.

P.K. Rol

49a

A molecular beam apparatus donated by NASA has been used to measure intermolecular potentials required as input for close coupled calculations of excitation cross sections.

Apparent cross sections for different energies are determined by measuring the attenuations of a fast (50 - 2500 eV) atom beam in passing through a scattering gas. The interaction potential is calculated from these cross sections and the scattering geometry.

The molecular beam apparatus used in this experiment is shown in Fig. IVa. Atomic ions are produced in the ion source. The ion beam is analyzed and the selected ions are forcused, collimated and decellerated to the required energy prior to neutralization in a charge exchange chamber. Just before entering the charge exchange chamber the ion beam is deflected to prevent high energy neutrals, formed by neutralization with the background gas, to be mixed with lower energetic atoms. The neutralized beam is finally passed through the scattering chamber and detected with a channel tron multiplier. The beam intensity is measured as a function of the scattering gas pressure, and the cross sections S can be calculated according to:

$$S = - \frac{1}{n\ell} \ln\left(I/I_0 \right)$$

Where I = attenuated beam flux.

I_0 = incident beam flux.

n = scattering gas density.

n ℓ = path length in scattering gas.

The equipment was tested by measuring the He-He potential for which accurate theoretical calculations are available. Excellent agreement was obtained with these theoretical results.

The repulsive potentials for oxygen atoms and several atoms and molecules have been calculated from measured incomplete scattering cross sections of fast-atom beams. These fast beams were produced by neutralizing either positive or negative 0-ion beams in a charge exchange gas. H_2O, Xe, O_2 and Kr were used as charge exchange gases.

The results are given in the form of Born-Mayer potentials in the following table.

Oxygen-atom Potentials

$$Ae^{-br} \qquad r_1 < r < r_u$$

A in eV
b in $\AA^{-1}$
r_1, r_u in $\AA$

Species	A	b	r_1	r_u	Exchange Reactions
N_2	569	3.044	1.20	2.37	O^+, H_2O
CO	837	3.297	1.25	2.32	O^+, H_2O
CO_2	2055	3.253	1.57	2.64	O^+, H_2O
H_2	500	4.058	0.865	1.75	O^+, Xe
NO	1037	3.348	1.30	2.35	O^+, Xe
H_2O	1415	3.700	1.27	2.22	O^+, Xe
O_2	1698	3.619	1.36	2.32	O^+, Xe
He	355	3.728	0.833	1.80	O^-, O_2
Ne	1415	3.984	1.18	2.06	O^-, O_2
Ar	745	3.184	1.25	2.36	O^-, O_2
Kr	1040	3.239	1.34	2.43	O^-, O_2
Xe	1470	3.303	1.44	2.50	O^-, O_2
He	360	3.702	0.844	1.82	O^+, Xe
Ne	1312	3.988	1.10	2.04	O^+, Xe
Ne	1125	3.864	1.15	2.06	O^+, Kr

In addition the incomplete cross sections have been measured
for the following combinations and potentials are being cal-
culated:

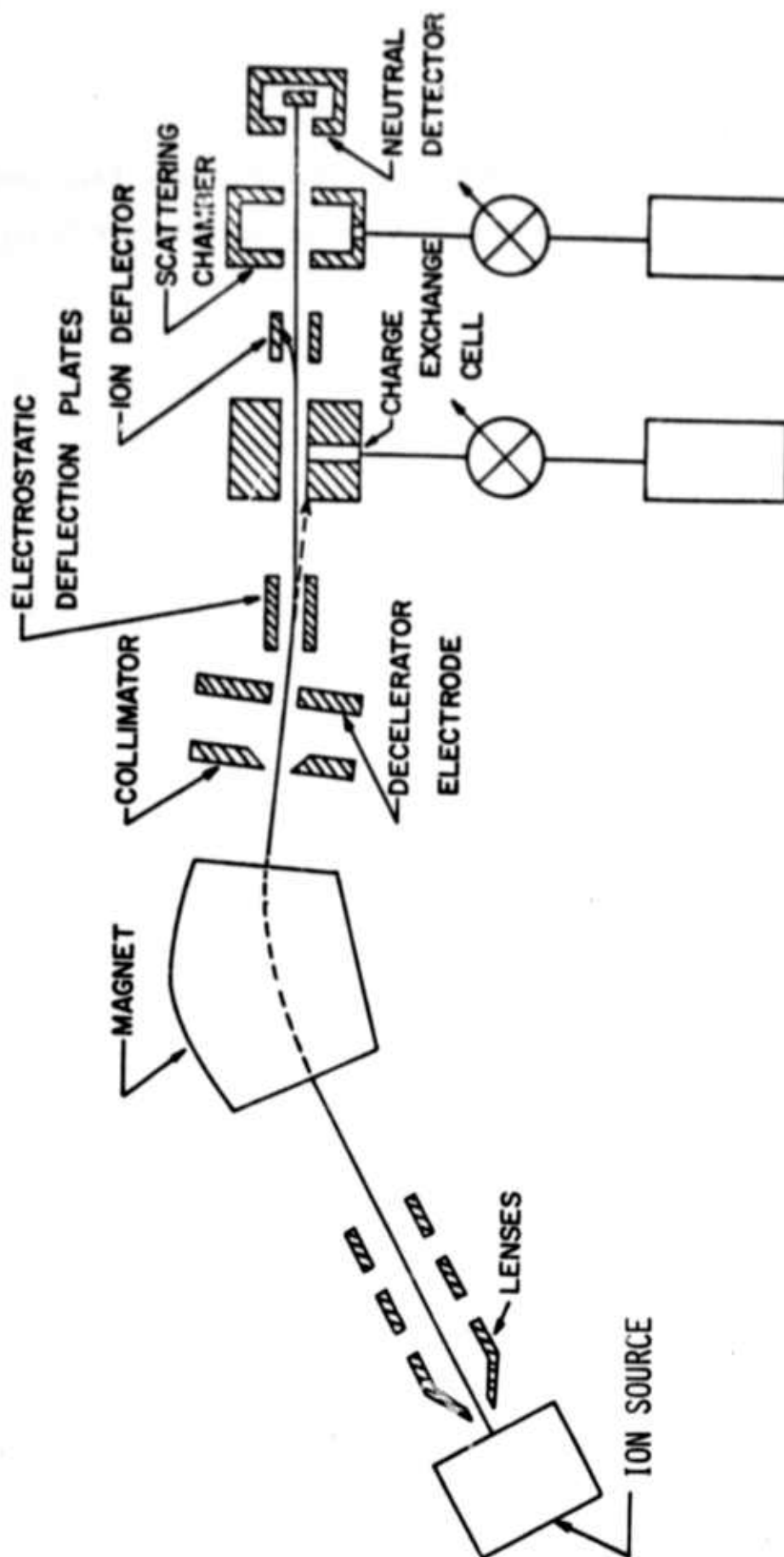| He-He	Ne-Ne	Ar-Ar	Kr-Kr	Xe-Xe
He-Ne	Ne-Ar	Ar-Kr	Kr-Xe	
He-Ar	Ne-Kr	Ar-Xe		
He-Kr	Ne-Xe			
He-Xe				

and H-He, D-He.

Figure IVa. Amdur-type molecular beam apparatus at Wayne State.